Title

Neonatal LPS exposure results in ATP8A2 down-regulation in the prefrontal cortex and depressive-like behaviors in mice through increasing IFN-γ level

Authors

Jiapeng Deng (ORCID: 0000-0002-0332-9296)[a] , Linyang Song (ORCID: 0000-0002-2770-9568)[b], Zhiqin Yang (ORCID: 0000-0002-3120-5944)[c], Sixie Zheng (ORCID: 0000-0001-6603-7947)[d], Zhuolin Du (ORCID: 0000-0003-0928-4081)[d], Li Luo[b,e], Jing Liu[b] , Xiaobao Jin[e], Junhua Yang (ORCID: 0000-0001-8037-9644)[b,e*]

Affiliations

[a] Class 1, Grade 2018, School of Clinical Medicine, Guangdong Pharmaceutical University, Guangzhou, Guangdong, People's Republic of China.

[b] Department of anatomy, School of Biosciences & Biopharmaceutics, Guangdong Pharmaceutical University, Guangzhou, Guangdong, People's Republic of China.

[c] Aviation health center, China southern airlines company limited, Guangzhou, Guangdong, People's Republic of China.

[d] Class 4, Grade 2018, School of Clinical Medicine, Guangdong Pharmaceutical University, Guangzhou, Guangdong, People's Republic of China.

[e] Guangdong Key Laboratory of Pharmaceutical Bioactive Substances, Guangdong Pharmaceutical University, Guangzhou, Guangdong, People's Republic of China.

Corresponding author

*Correspondence should be addressed to Junhua Yang at the following address, phone, and email address:

Address: Junhua Yang, Room 510#, Building of Basic Medical Sciences, School of Biosciences & Biopharmaceutics, Guangdong Pharmaceutical University, No. 230, East Waihuan Street, Higher Education Mega Center, Guangzhou City, Guangdong Province, Postcode 510006, P. R. China.

Tel.: + 86 20 39352189.

E-mail: jhyang2018@gdpu.edu.cn.

Abstract

Neonatal lipopolysaccharide (LPS) exposure can lead to depressive-like behaviors in mice through inducing pro-inflammatory cytokines including interferon(IFN)-γ. ATP8A2 is a phospholipid transporter located on the cell membrane. Studies have shown that the decrease in ATP8A2 expression in the prefrontal cortex (PFC) is associated with depressive behavior. Moreover, it has been reported that IFN-γ could reduce ATP8A2 expression in non-neuronal cells. These findings prompted us to hypothesize that neonatal LPS exposure might induce ATP8A2 down-regulation in PFC in mice by increasing the IFN-γ level. Mice pups consisting approximately evenly of both sexes were intraperitoneally injected with 3 doses of LPS (50 μg/kg body weight for each dose) on postnatal day (PND5), PND7 and PND9. Here, we first found that PFC ATP8A2 expression decreased significantly and transiently till ten days after neonatal LPS exposure with the lowest level at two days after it. Moreover, a negative correlation of PFC ATP8A2 expression was found with the PFC level of IFN-γ, rather than the other LPS-induced pro-inflammatory cytokines. Using anti-IFN-γ neutralizing mAb, IFN-γ was identified as the key mediator of LPS-induced ATP8A2 down-regulation in PFC in mice. Besides, neutralizing IFN-γ partially but significantly rescued the depressive-like behaviors in adulthood induced by neonatal LPS exposure. In sum, the present study showed that neonatal LPS exposure induced ATP8A2 down-regulation in PFC and depressive-like behaviors in mice through increasing the IFN-γ level.

Keywords: Neonatal period; Lipopolysaccharide/LPS; Interferon-γ/IFN-γ; ATP8A2; prefrontal cortex/PFC; Depression

Introduction

ATP8A2, a member of the P4-ATPase family in mammals, is highly expressed in the brain, spinal cord, testis, and retina, which flipping phosphatidylserine and phosphatidylethanolamine across the cell membrane (Andersen et al., 2016). It plays an important role in maintaining the stability and normal function of the cell membrane (Coleman et al., 2009). Therefore, ATP8A2 in the brain is vital for normal neural development and function (Coleman and Molday, 2011; Xu et al., 2012), since these processes involve cell proliferation, migration, synapses pruning of neurons (Brandon and Sawa, 2011). ATP8A2 expressed in the brain has received extensive attention recently and researches have shown that reduced expression of ATP8A2 leads to axonal mutation and neurodegenerative diseases (Choi et al., 2019; Zhu et al., 2012). There is also research reporting that ATP8A2 expression decreases in conditions of Alzheimer's disease and bacterial infection (Aaron et al., 2018; Ross et al., 2011). Moreover, depressive-like behavior has been reported to be associated with decreased ATP8A2 expression in the prefrontal cortex (PFC) (Chen et al., 2017). Although ATP8A2 has been widely studied, little is known about how ATP8A2 expression is regulated.

Recently, IFN-γ was shown to significantly reduce the expression of ATP8A2 in non-neuron cells (Shulzhenko et al., 2018). IFN-γ produced in the periphery can

86 penetrate brain parenchyma across the immature blood-brain barrier and even increase
87 the permeability of the mature blood-brain barrier (Hansen-Pupp et al., 2005; Wong et
88 al., 2004). IFN-γ may mediate the neonatal lipopolysaccharide (LPS)
89 exposure-induced depressive-like behaviors in mice (Campos et al., 2014), which is
90 associated with the function of PFC. Besides, IFN-γ expression in PFC increased
91 more than twice after LPS treatment (Laumet et al., 2018). Based on the background
92 mentioned above, it was postulated that neonatal LPS exposure might induce ATP8A2
93 down-regulation in PFC in mice by increasing the IFN-γ level. There is yet no report
94 addressing this issue.

95 To test this hypothesis, we challenged neonatal mice with LPS and observed a
96 transiently decreased expression of ATP8A2 in PFC. Using a series of experiments,
97 we further identified IFN-γ as the key mediator of LPS-induced ATP8A2
98 down-regulation in PFC in mice. These findings may reveal a potential mechanism by
99 which early inflammation leads to impairment of the central nervous system
100 development and function.

101

102 **2. Materials and methods**

103 *2.1. Animals designing*

104 Litters of newborn C57BL6/J mice (one-day-old) consisting approximately evenly
105 of both sexes were ordered together with their mothers from Guangdong Medical
106 Laboratory Animal Center (Guangzhou, China). They were housed in a specific

pathogen-free condition under 12 h light-12 h dark conditions with food and water available ad libitum.

In this study, a randomized block design was used to minimize the effects of systematic error according to publications by statisticians who stated that if the experimenters aim to focus exclusively on the differences between/among different treatment conditions, the effects due to variations between the different blocks should be eliminated by using a randomized block design ANOVA (Refer to https://doi.org/10.1007/978-0-387-32833-1_344; http://www.r-tutor.com/elementary-statistics/analysis-variance/randomized-block-design). In such design, there is only one primary factor under consideration in the experiment. Similar test subjects are grouped into blocks. Then, subjects within each block are randomly assigned to treatment conditions. Each block is tested against all treatment levels of the primary factor at random order. Thus, possible influence by other extraneous factors will by eliminated.

To be specific, a randomized block design was conducted for each of the experiments for investigating potential differences between or among treatment conditions. Each of the blocks consisted of two (for experiments reported in Fig.1 and Fig.2), three (for experiment reported in Fig.5) or five (for experiments reported in Fig.4 and Fig.6) same-sex pups from a same dam. The pups in each block were randomly assigned to different treatment conditions (only one pup in each block for receiving each kind of the different treatment conditions). The sex of n pups in different blocks were same or different, while the litter background of pups in

different blocks were certainly different The detailed information indicating how many litters were used and how many pups from each litter were included in each group of each experiment in this study were shown in Supplementary talbe1 to table6 (Supplementary Material). Pups subjected to behavioral tests were weaned on postnatal day (PND)21. Pups subjected to other tests were sacrificed on PND11. This study was approved by the Institutional Animal Ethics Committee of Guangdong Pharmaceutical University.

2.2. LPS treatment

Mice were intraperitoneally injected with 3 doses of LPS dissolved in 0.1 mol phosphate balanced solution (PBS) (Escherichia coli O111: B4; Sigma-Aldrich) (50 μg/kg bodyweight for each dose;) on PND5, PND7 and PND9. The dosage and schedule for LPS injection were determined based on previous studies (Dinel et al., 2014; Doosti et al., 2013; Liang et al., 2019). The experiment was controlled by intraperitoneal injection of PBS. Littermates were toe-clipped for identification randomly assigned to each of the groups in each experiment as described in Results.

2.3 Administration of anti-IFN-γ neutralizing mAb and an isotype IgG1

For experiments conducted in this study as reported in Section 3.3 and Fig.4 to Fig.6, anti-IFN-γ neutralizing mAb and/or an isotype IgG1 (Invitrogen, Thermo Fisher Scientific, Waltham, MA, USA) were intraperitoneally injected daily to mice from PND5 to PND10. By a special experiment, the optimal dosage was first

149 determined as 0.6 mg/kg body weight of anti-IFN-γ neutralizing mAb. The dosage of
150 isotype IgG1 was determined as 0.6 mg/kg body weight accordingly.

151 *2.4 Western blot*

152 After being over-anesthetized with 10% chloral hydrate, the mice were decapitated
153 and killed. The mouse PFC tissues were immediately taken on ice, and then
154 homogenized in RIPA lysate containing protease inhibitors (Beyotime, Wuhan,
155 China). After centrifuged at 13000g for 30 min at 4°C, the supernatant was taken. The
156 BCA protein analysis method was used to determine the total protein content of the
157 sample. After mixed with 5×SDS-PAGE loading buffer at the volume ratio of V
158 (protein sample solution): V (5×SDS-PAGE Loading Buffer) = 4:1, the samples were
159 boiled and denatured for 5 min, save for later use. The samples of each group were
160 subjected to SDS polyacrylamide gel electrophoresis. The gel used here is a
161 simplified hand-poured gradient gel, in which the ratio was 40% of the volume being
162 6% acrylamide and 60% of the volume being 12% acrylamide (using an SDS-PAGE
163 Gel Quick Preparation Kit, Beyotime, Shanghai, China). The procedure to make this
164 gradient gel was according to a previous study (Miller et al., 2016) with modification
165 with respect to the concentrations of acrylamide. When proteins were transferred to
166 PVDF membranes, the membranes were cut according to the indication of the color
167 marker (10-180 kDa, ThermoFisher, Shanghai, China). Two parts of each membrane,
168 one located in the marker's range 70-180 kDa and the other in the range 25-55 kDa,
169 containing the target proteins ATP8A2 (129 kDa) and the internal control proteins
170 β-actin (43 kDa) were subjected to the subsequent treatment. These membranes were

blocked with 5% skimmed milk powder at RT for 2 h. After this, these membranes were put into the corresponding primary antibody incubation solutions, one containing anti-ATP8A2 antibodies (1:500, Abcam, Cambridge, MA, USA) and the other containing anti-β-actin antibodies (1:5000, Abcam, Cambridge, MA, USA) and incubated at 4°C overnight. After rinsing with TBST, these membranes were put into the corresponding secondary antibodies incubation solutions, one containing horseradish peroxidase (HRP)-conjugated goat anti-rabbit antibodies (1:5000, Bioworld, Atlanta, GA, USA) and the other containing HRP-conjugated goat anti-rabbit antibodies (1:5000, Bioworld, Atlanta, GA, USA) and incubated at RT for 1 h. After rinsing with TBST, ECL luminescent solution is added on the membranes in a dark room for exposure and development. Chemiluminescent images were obtained with Carestream XBT X-ray Film (Rayco, Xiamen, Fujian, China), and subsequently scanned and quantified by densitometry using ImageJ software.

2.5 Determination of cytokines levels

Forty-eight h after the last LPS injection, the mice were anesthetized deeply with 10% chloral hydrate before the blood was collected from the heart immediately. After blood collection, it was allowed to stand at room temperature for 1 h, and after centrifugation, the supernatant was taken and stored at -70°C for the experiment. Then the mice were transcranial perfused with 0.9% NaCl and PFC was collected immediately on ice. A mouse cytokine/chemokine magnetic bead panel (MCYTOMAG-70K-06; Millipore, Billerica, MA, USA) was employed to detect the levels of IFN-γ, tumor necrosis factor (TNF)-α, interleukin(IL)-1β, IL-6 both in the

serum and PFC (Yang et al., 2016). Each of the serum samples was diluted at 1:2 in assay buffer. PFC tissue was prepared as homogenates before assayed. The total protein concentration of each sample was adjusted to 4.5 mg/ml using a BCA protein assay kit (Beyotime, Shanghai, China). Then, the prepared serum and PFC samples were used strictly according to the manufacturer's protocols for the multiplex assays. The data were collected on a Bio-Plex-200 system (Bio-Rad, Hercules, CA, USA) and analyzed using professional software (Bio-Plex Manager).

2.6 Immunofluorescence and cell quantification

Forty-eight h after the last LPS injection, the mice were over-anesthetized with 10% chloral hydrate and transcranial perfused with 0.9% NaCl followed by 4% paraformaldehyde (PFA). After removed, the brains were immediately post-fixed in 4% PFA overnight at 4 °C. Then, the brains were gradient dehydrated with 10%, 20%, and 30% sucrose for 24 h each at 4°C. Free-floating, serial coronal sections (40 μm) were collected on a Leica SM2000R freezing microtome (Leica Microsystems, Richmond Hill, Ontario, Canada) and stored at 4°C for immunostaining. Sections were washed in PBS three times and then blocked in PBS containing 1% bovine serum albumin (BSA) and 0.25% Triton X-100 (Sigma-Aldrich, St. Louis, MO, USA) for 1 h at 37°C. The slices were then incubated in the primary antibodies overnight at 4°C. The primary antibodies, including rabbit anti-ATP8A2 (1:200; Abcam, Cambridge, MA, USA) and mouse anti-NeuN (1:1000; Abcam, Cambridge, MA, USA), were diluted in PBS containing 1% BSA and 0.25% Triton X-100. Afterward, the specimens were washed three times in PBS and then were incubated with

secondary antibodies, including Alexa Fluor 555-conjugated goat anti-rabbit and Alexa Fluor 488-conjugated donkey anti-mouse for 2 h at 37°C. Both secondary antibodies (Invitrogen, Thermo Fisher Scientific, Waltham, MA, USA) were diluted to 1:400.

A Stereo Investigator stereological system (MicroBrightField, Williston, USA) was used for quantitative analyses of the ATP8A2$^+$ cells in the unilateral PFC of each mouse. Coronal sections of the PFC were collected through the rostrocaudal axis spanning approximately from +3.20 mm to +2.10 mm relative to bregma (Xiong et al., 2017)to count the interested cells. Measurements were recorded from an equidistant series of six coronal sections. After the actual section thickness was measured, appropriate guard zones at the top and bottom of each section were defined to avoid oversampling. The 40× objective of a Nikon microscope was used for all stereological analyses. The numbers of ATP8A2$^+$/NeuN$^+$ and NeuN$^+$ cells within the traced region (PFC) in each of the six selected sections were straightly quantified without using a grid or counting frames. A Zeiss LSM780 confocal laser-scanning microscope (Carl Zeiss AG, Oberkochen, Germany) was used to capture the representative confocal micrographs of the labeled cells.

For ATP8A2 in situ densitometric analysis, one 40-μm-thick coronal section at the middle of the PFC (+2.10 mm relative to bregma) was collected from each animal. Single labeling for ATP8A2 immunofluorescently was performed, rather than double labeling for ATP8A2/NeuN, to minimize the possible interference with ATP8A2 positive immunofluorescence signal intensity during staining practice. A Zeiss

LSM780 confocal laser-scanning microscope (Carl Zeiss AG, Oberkochen, Germany) was used to capture the micrographs of the same field as the double-labeled micrographs shown in Fig.6D-F. The ATP8A2 signal was measured as a mean gray value using the software ImageJ and the data were shown in Fig.6 as a relative influence. The procedures were: 1) Image-Type-8bit; 2) Image-Adjust-Threshold; 3) Image-Adjust-Auto Threshold; 4) Analyze-Set Measurements; 5) Analyze-Measure.

2.7. Forced swim test (FST)

FST is a standard test used as a screen for measuring depressive-like behaviors in mice. The experiment was carried out on the PND90, the mice were brought to the laboratory one week in advance to let them adapt to the environmental room. In this experiment, mice were placed in a plastic cylinder (40 cm in-depth, 20 cm in diameter and filled with water at 24±°C with the water's height at 25 cm above from the bottom. Each mouse was put in the plastic cylinder in the same way and forced to swim for 6 min in the plastic cylinder. The first two minutes of mouse behavior was not recorded. The following 4 minutes were recorded by a video tracking system EthoVision (Noldus Information Technology B.V., Wageningen, Netherlands) for the analysis of the total time spent by each animal in staying on the water surface without any struggling or swimming during the test. At the end of the experiment, the hair of the mice was blown dry to prevent them from catching a cold.

2.8 Tail-suspension test (TST)

TST is also one of the most commonly used experiments to evaluate depressive-like behavior in rodent models. In the present study, TST was performed on the second day after the FST. During this test, each mouse was held below its tail to the edge of the clip and suspended 60 cm above from the floor. The performances of mice were recorded by a video tracking system EthoVision (Noldus Information Technology B.V., Wageningen, Netherlands) four minutes with a 2-min-gap left prior to the recording. The total time spent by each animal in not struggling during the test was analyzed. After all behavioral tests were done, animals were killed by over-anesthetized with 10% chloral hydrate.

2.9 Statistical analyses

The data were statistically analyzed using the SPSS 25.0 statistical software (Chicago, IL, USA). *Pearson*'s correlation analysis was used for data shown in Fig.3. Data shown in Fig.1, Fig.2, Fig.4, Fig.5 and Fig.6 were statistically analyzed using a randomized block design ANOVA to account for the effects of treatment (such as LPS injection and/or anti-IFN-γ neutralizing mAb injection) by modeling both litter factor and sex factor as a fixed effect described as "block effect" in section Results and the treatment factor as a random effect described as "treatment effect" in section Results. For data obtained from more than two treatment groups, the performance of randomized block design ANOVA were followed by Tukey's *post hoc* test. *P* values are displayed as follows: n.s. = not significant, * $p < 0.05$, ** $p < 0.01$, *** $p < 0.001$.

3. Results

3.1 Neonatal LPS exposure induced a transiently down-regulated expression of ATP8A2 in the PFC in mice

To determine whether neonatal LPS exposure influence the expression of ATP8A2 in the PFC in mice and how long this potential influence would last following LPS exposure, the first experiment was carried out. Mice in the LPS group were injected with LPS and those in the CON group with PBS of the same volume. Two groups of mice were sacrificed after 1 day, 2 days, 4 days, or 10 days after the last LPS injection. The left unilateral PFC tissue from every mouse was taken on ice to be homogenated immediately for Western blot analyses of ATP8A2 level. The right unilateral PFC tissue was taken on ice and stored at -70°C at once for ELISA analyses of LPS-induced pro-inflammatory cytokines if necessary.

As shown in Fig.1, the ATP8A2 levels significantly decreased at the former three test time points: 1 day (randomly block design ANOVA, block effect: $F_{(5,5)} = 1.122$, $p = 0.451$, $n = 6$; treatment effect: $F_{(1,5)} = 44.815$, $p = 0.001$, $n = 6$), 2 days (randomly block design ANOVA, block effect: $F_{(5,5)} = 0.785$, $p = 0.601$, $n = 6$; treatment effect: $F_{(1,5)} = 77.139$, $p < 0.001$, $n = 6$) and 4 days (randomly block design ANOVA, block effect: $F_{(5,5)} = 0.810$, $p = 0.588$, $n = 6$; treatment effect: $F_{(1,5)} = 37.270$, $p = 0.002$, $n = 6$) after the last LPS injection. However, such decrease was no longer detectable 10 days after the last LPS injection (randomly block design ANOVA, block effect: $F_{(5,5)} = 0.489$, $p = 0.775$, $n = 6$; treatment effect: $F_{(1,5)} = 0.077$, $p = 0.792$, $n = 6$) (Fig.1). It

299 is worth noting that the largest extent of the decrease in PFC ATP8A2 expression was
300 observed in the sample obtained 48 h after the last LPS injection (Fig.1). These
301 findings verified the expected influence of neonatal LPS exposure on the PFC
302 ATP8A2 expression in mice and revealed the time curve of PFC ATP8A2 expression
303 following neonatal LPS exposure.

304 *3.2 PFC ATP8A2 level was only significantly correlated to IFN-γ level among all four*
305 *elevated pro-inflammatory cytokines both in serum and in the PFC*

306 Given the initial finding that PFC ATP8A2 expression was reduced to the largest
307 extent 48 h after the last LPS injection (Fig.1), the prepared serum and PFC samples
308 (n = 6) obtained at the same time point in the last experiment were then subjected to
309 ELISA analyses for the levels of LPS-induced pro-inflammatory cytokines, including
310 IFN-γ, IL-1β, IL-6and TNF-α.

311 Moreover, another experiment was performed in which the animal was treated all
312 the same way and the levels of PFC ATP8A2 as well as the levels pro-inflammatory
313 cytokines both in the serum and PFC were detected specifically 48 h after the last LPS
314 injection, using a larger sample size (n = 9) so as both to provide a repetitive
315 verification of the very novel finding of ATP8A2 in the brain and to make the total
316 sample size up to n = 15 (together with n = 6) for this chosen test time point.
317 *Pearson*'s correlation analysis between PFC ATP8A2 level and the level of each of
318 the LPS-induced pro-inflammatory cytokines would get good confidence in the case
319 of n = 15.

As shown in Fig.2A-B, the PFC ATP8A2 level decreased by more than 90% in LPS group (randomly block design ANOVA, block effect: $F_{(8,8)} = 1.166$, $p = 0.417$, $n = 9$; treatment effect: $F_{(1,8)} = 3.993$, $p < 0.001$, $n = 9$). All the detected cytokines, whether in serum (Fig.2C-F) or in PFC (Fig.2G-J), showed a dramatically increased expression (Serum IL-6: randomly block design ANOVA, block effect: $F_{(8,8)} = 0.999$, $p = 0.500$, $n = 9$; treatment effect: $F_{(1,8)} = 212.013$, $p < 0.001$, $n = 9$. serum IFN-γ: randomly block design ANOVA, block effect: $F_{(8,8)} = 1.098$, $p = 0.449$, $n = 9$; treatment effect: $F_{(1,8)} = 37.708$, $p < 0.001$, $n = 9$; serum IL-1β: randomly block design ANOVA, block effect: $F_{(8,8)} = 1.053$, $p = 0.472$, $n = 9$; treatment effect: $F_{(1,8)} = 93.958$, $p < 0.001$, $n = 9$; serum TNF-α: randomly block design ANOVA, block effect: $F_{(8,8)} = 0.952$, $p = 0.527$, $n = 9$; treatment effect: $F_{(1,8)} = 181.681$, $p < 0.001$, $n = 9$; PFC IFN-γ: randomly block design ANOVA, block effect: $F_{(8,8)} = 1.145$, $p = 0.427$, $n = 9$; treatment effect: $F_{(1,8)} = 134.25$, $p < 0.001$, $n = 9$; PFC IL-1β: randomly block design ANOVA, block effect: $F_{(8,8)} = 1.668$, $p = 0.243$, $n = 9$; treatment effect: $F_{(1,8)} = 62.695$, $p < 0.001$, $n = 9$; PFC IL-6: randomly block design ANOVA, block effect: $F_{(8,8)} = 0.990$, $p = 0.505$, $n = 9$; treatment effect: $F_{(1,8)} = 184.902$, $p < 0.001$, $n = 9$; PFC TNF-α: randomly block design ANOVA, block effect: $F_{(8,8)} = 0.995$, $p = 0.503$, $n = 9$; treatment effect: $F_{(1,8)} = 105.007$, $p < 0.001$, $n = 9$)

Taken all the data from 48 h time point samples from LPS-treated mice together, *Pearson*'s correlation analysis was performed between PFC ATP8A2 level and the level of each of the LPS-induced pro-inflammatory cytokines ($n = 15$). There was a significant negative correlation between ATP8A2 expression in PFC and IFN-γ level

both in serum ($p < 0.01$, *Pearson*'s correlation analysis, $n = 15$) (Fig.3 A) and in PFC ($p < 0.001$, *Pearson*'s correlation analysis, $n = 15$) (Fig.3E). No significant correlations were found between ATP8A2 level and all the other pro-inflammatory cytokines (all p values > 0.05) (Fig.3 B-D, F-H). These results suggest that IFN-γ plays an important role in the PFC ATP8A2 down-regulation caused by neonatal LPS exposure.

3.3 IFN-γ mediated the PFC ATP8A2 down-regulation caused by neonatal LPS exposure

To further explore the potential role of IFN-γ in mediating the PFC ATP8A2 down-regulation following neonatal LPS exposure, an IFN-γ-blocking experiment was conducted using anti-IFN-γ neutralizing mAb and an isotype IgG1. Before this IFN-γ-blocking experiment, another experiment was carried out to determine the optimal dosage of anti-IFN-γ neutralizing mAb. The dosage of 0.6 mg/kg body weight restored the IFN-γ levels to normal physiological levels both in serum (randomly block design ANOVA, block effect: $F_{(7,35)} = 0.449$, $p = 0.864$, $n = 8$; treatment effect: $F_{(5,35)} = 78.511$, $p < 0.001$, $n = 8$; *post hoc test*, LPS+anti-IFN-γ(0.6) group vs. CON group: $p = 1.000$) (Fig.4A) and in PFC (randomly block design ANOVA, block effect: $F_{(7,35)} = 0.718$, $p = 0.657$, $n = 8$; treatment effect: $F_{(5,35)} = 35.571$, $p < 0.001$, $n = 8$; *post hoc test*, LPS+anti-IFN-γ(0.6) group vs. CON group: $p = 0.835$) (Fig.4B). Then, we proceeded to the IFN-γ-blocking experiment and five groups of mice were set. To be specific, the CON group and LPS group were set as above. LPS+anti-IFN-γ(0.6) group was set by injecting LPS combined with anti-IFN-γ neutralizing mAb. The

LPS+IgG1 group was set by injecting LPS combined with an isotype IgG1. The last group was set by injecting mere anti-IFN-γ neutralizing mAb (anti-IFN-γ(0.6)).

Randomly block design ANOVA revealed significant differences in IFN-γ levels among five groups (Fig.4C, serum IFN-γ level: randomly block design ANOVA, block effect: $F_{(7,28)} = 0.611$, $p = 0.742$, $n = 8$; treatment effect: $F_{(4,28)} = 52.664$, $p < 0.001$, $n = 8$) (Fig.4D, PFC IFN-γ level: randomly block design ANOVA, block effect: $F_{(7,28)} = 0.276$, $p = 0.958$, $n = 8$; treatment effect: $F_{(4,28)} = 95.875$, $p < 0.001$, $n = 8$). We first confirmed that administration of anti-IFN-γ neutralizing mAb blocked the increase of IFN-γ levels both in systemic blood (LPS+anti-IFN-γ(0.6) group vs. CON group: $p = 0.998$) (Fig.4C) and PFC (LPS+anti-IFN-γ(0.6) group vs. CON group: $p = 0.903$) (Fig. 4D), while isotype IgG1 failed to block the LPS-induced IFN-γ increase either in serum (LPS+IgG1 group vs. CON group: $p < 0.001$; LPS+IgG1 group vs. LPS group: $p = 0.976$) (Fig.4C) or in PFC (LPS+IgG1 group vs. CON group: $p < 0.001$; LPS+IgG1 group vs. LPS group: $p = 0.563$) (Fig.4D). In the absence of LPS exposure, the anti-IFN-γ neutralizing mAb significantly neutralized the physiological IFN-γ both in blood (anti-IFN-γ(0.6) group vs. CON group: $p = 0.013$; LPS+IgG1 group vs. LPS group: $p = 1$) (Fig.4C) and in brain of mice (anti-IFN-γ(0.6) vs. CON group: $p < 0.001$; LPS+IgG1 group vs. LPS group: $p = 1$) (Fig.4D).

Randomly block design ANOVA of Western blot data revealed significant differences in PFC ATP8A2 levels among five groups (Fig.4E, randomly block design ANOVA, block effect: $F_{(7,28)} = 1.273$, $p = 0.099$, $n = 8$; treatment effect: $F_{(4,28)} = 122.582$, $p < 0.001$, $n = 8$). We found that neutralization of IFN-γ blocked the

386 LPS-induced ATP8A2 decrease in PFC (LPS+anti-IFN-γ(0.6) group vs. CON group:
387 $p = 1$) (Fig.4E-F), while the isotype IgG1 showed no significant blocking effect on the
388 LPS-induced ATP8A2 decrease in PFC (LPS+IgG1 group vs. LPS group: $p = 0.923$;
389 LPS+IgG1 group vs. LPS+anti-IFN-γ(0.6) group: $p < 0.001$) (Fig.4E-F). Interestingly,
390 in the absence of LPS exposure, mere anti-IFN-γ neutralizing mAb administration led
391 to no significant influence on the PFC ATP8A2 level (anti-IFN-γ(0.6) group vs. CON
392 group: $p = 1$) (Fig.4E-F), although it neutralized the physiological IFN-γ both in the
393 blood (Fig.4C) and in the brain of mice (Fig.4D).

394 We next performed another experiment to observe the role of IFN-γ using
395 immunofluorescence detection, with a total of three groups set, CON group, LPS
396 group, and LPS+anti-IFN-γ(0.6) group. The groups by giving isotype IgG1 or mere
397 anti-IFN-γ neutralizing mAb were no longer set due to the confirmed results shown
398 above. The results of randomly block design ANOVA of immunofluorescence
399 detection of PFC ATP8A2 levels showed similar findings to Western blot.
400 Neutralization of IFN-γ blocked the LPS-induced ATP8A2 decrease in PFC, indicated
401 by the mean fluorescence intensity (randomly block design ANOVA, block effect:
402 $F_{(5,10)} = 0.472$, $p = 0.789$, $n = 6$; treatment effect: $F_{(2,10)} = 47.016$, $p < 0.001$, $n = 6$;
403 *post hoc test*, LPS+anti-IFN-γ(0.6) group vs. CON group: $p = 0.849$) (Fig.5K) and
404 $ATP8A2^{+}/NeuN^{+}$ cells (randomly block design ANOVA, block effect: $F_{(5,10)} = 0.121$,
405 $p = 0.985$, $n = 6$; treatment effect: $F_{(2,10)} = 47.016$, $p < 0.001$, $n = 6$; *post hoc test*,
406 LPS+anti-IFN-γ(0.6) group vs. CON group: $p = 0.532$) (Fig.5L). Besides, there were
407 no significant differences among three groups in the number of neurons ($NeuN^{+}$ cells)

in PFC (data are not shown) although nearly all patchy ATP8A2^{+} signals were co-located with NeuN^{+} signals (Fig.5G-I). The findings shown in this section identified IFN-γ as the key mediator of the PFC ATP8A2 down-regulation caused by neonatal LPS exposure. Moreover, ATP8A2 alterations were not accompanied by a detectable change in the number of neurons (NeuN^{+} cells) in PFC.

3.4 IFN-γ plays an important role in depressive-like behaviors in adulthood induced by neonatal LPS exposure

Abnormality in PFC, especially during the critical development period, is an important pathophysiological basis of depression and it has been verified that *neonatal LPS exposure* could result in depression in adulthood (Dinel et al., 2014; Walker et al., 2013). Therefore, we investigated whether neutralization of IFN-γ affects the behavioral performances in the FST and TST of the LPS-treated mice. The floating immobility time was partially restored toward the levels of CON group both in FST task (randomly block design ANOVA, block effect: $F_{(11,44)} = 0.825$, $p = 0.616$, $n = 12$; treatment effect: $F_{(4,44)} = 36.675$, $p < 0.001$, $n = 12$; *post hoc test*, LPS+anti-IFN-γ(0.6) group vs. CON group: $p < 0.001$) (Fig.6A) and in TST task (randomly block design ANOVA, block effect: $F_{(11,44)} = 0.949$, $p = 0.504$, $n = 12$; treatment effect: $F_{(4,44)} = 35.619$, $p < 0.001$, $n = 12$; *post hoc test*, LPS+anti-IFN-γ(0.6) group vs. CON group: $p < 0.001$) (Fig.6B).

The isotype IgG1 failed to block the LPS-induced behavioral alterations either in FST (LPS+IgG1 group vs. CON group: $p < 0.001$; LPS+IgG1 group vs. LPS group: p

= 0.240) (Fig.6A) or in TST (LPS+IgG1 group vs. CON group: $p < 0.001$; LPS+IgG1 group vs. LPS group: $p = 0.770$) (Fig.6B). In the absence of LPS exposure, the anti-IFN-γ neutralizing mAb led to no significant behavioral alterations in FST (anti-IFN-γ(0.6) group vs. CON group: $p = 0.984$; LPS+IgG1 group vs. LPS group: $p = 0.770$) (Fig.6A) or in TST (anti-IFN-γ(0.6) vs. CON group: $p = 0.617$) (Fig.6B). These results suggested an important role of IFN-γ in depressive-like behaviors in adulthood induced by neonatal LPS exposure.

3.5 No sex dimorphism in ATP8A2 levels despite a sex dimorphism in depressive-like behaviors in mice

All the analyses described above were intended to exclusively detect the effects of different treatment conditions to test the hypothesis that neonatal LPS exposure might influence PFC ATP8A2 expression in mice involving an increased IFN-γ level and therefore the sex factor was not under consideration as stated in section 2.1. However, previous studies showed that sex may affect immune activation (Cai et al., 2016). So, we also analyzed the data collected from the experiments in section 3.1 and 3.2 shown in Fig.2 as well as in the bars in Fig.1 indicated as day2 using another statistical method to observe whether there were significant differences in PFC ATP8A2 expression and the levels of proinflammatory cytokines between two sexes either in the presence of LPS challenge or not. The results showed no significant differences in the levels of these molecules between male and female animals either in the presence of LPS challenge or not (all p values > 0.05, see details in Supplementary Fig.1 and its legend). Furthermore, data collected from behavioral tests and shown in section 3.4

(Fig.6) were also subjected to additional analysis for differences between two sexes. The results showed no significant differences in the behavioral task performances between male and female animals either in the presence of LPS challenge or not (all p values > 0.05, see details in Supplementary Fig.2 and its legend).

Discussion

Our research revealed that the neonatal LPS exposure induced ATP8A2 down-regulation in PFC and depressive-like behaviors in mice by increasing the IFN-γ level. This finding, based on a series of studies concerning the influence of LPS on brain development and behavior (Bilbo and Schwarz, 2012; Doosti et al., 2013), is the first to report the change of ATP8A2 in the PFC in this animal model and the mechanism underlying how LPS affects PFC ATP8A2 expression. Moreover, this study further extends our understanding of the mechanism underlying behavioral effects of early immune activation.

Intraperitoneal LPS injection has been shown to cause a range of acute physiological, pathological, and psychological disorders in rodents. Impairments both in food intake and social exploratory behavior in rodents have been demonstrated in rodents administered intraperitoneally with LPS (Haba et al., 2012; O'Reilly et al., 1988). It has also been reported that LPS exposure can induce depressive and anxiety-like behaviors (Depino, 2015; Doosti et al., 2013). Moreover, LPS may reduce acutely the level of prefrontal cortical neurogenesis in adult rodents (Wang et al., 2016). The data from the LPS-treated mice in the present study enriched these

473 widely reported neurobehavioral impairments.

474 LPS challenge may induce a large extent release of cytokines both in the periphery
475 and brain, particularly pro-inflammatory cytokines, including IFN-γ, IL-1β, IL-6, and
476 TNF-α (Klimstra et al., 1999). These pro-inflammatory cytokines not only play an
477 important role in immunity but also may affect brain function and mediate
478 disease-like behaviors. For example, these pro-inflammatory factors have been shown
479 to cause depressive-like behavior in mice (Gupta et al., 2016; Hashimoto, 2015;
480 Kohler et al., 2014; Pokryszko-Dragan et al., 2012). The results of cytokines in our
481 study showed clearly that their levels in the periphery and the brain were highly
482 consistent. this fact may partially due to the immature blood-brain barrier or increased
483 permeability of it during inflammation.

484 ATP8A2 is a protein located in the membrane, functioning to transport
485 phosphatidylserine into the inner layer of membrane, and thus it is important to
486 maintain the structural stability and normal function of the membrane (Andersen et al.,
487 2016; Coleman et al., 2009). Since the distribution of ATP8A2 in the brain has been
488 determined recently (Andersen et al., 2016), little has been known about the potential
489 factors involved in the regulation of its expression. ATP8A2 expression
490 down-regulation has been observed in certain pathological conditions including
491 Alzheimer's disease and bacterial infection (Aaron et al., 2018; Ross et al., 2011).
492 However, the study reported a mechanism underlying such regulation could not be
493 seen so far. Decreased level of ATP8A2 in the PFC also occurs in the presence of
494 stress and depressive situation (Chen et al., 2017), but the causal relationship between

ATP8A2 change and behavior change is unclear. The current study revealed that ATP8A2 expression in the PFC could be down-regulated by a high concentration of IFN-γ, which is consistent with another study verifying that IFN-γ down-regulated the expression of ATP8A2 in non-neuron cells (Shulzhenko et al., 2018). This finding deepens the understanding of how depression is induced during infections by LPS-producing gram-negative bacteria.

LPS exposure can induce neuroinflammation in various brain regions and result in functional abnormalities, such as hippocampal neuroinflammation and impaired learning and memory (Lee et al., 2008; Shaw et al., 2001). In this study, the animal model that simulates a depressive-like phenotype caused by early bacterial infection was used to investigate whether LPS caused alteration in ATP8A2 expression. Therefore, PFC was selected as the brain region to observe ATP8A2 expression that it's the area of the brain mostly focused on by studies about depressive-like behavior (Myers-Schulz and Koenigs, 2012). In future studies, we will investigate the expression of ATP8A2 in other pathological conditions and/or in other brain zones such as the hippocampus.

As well-known, LPS-induced inflammation is transient. Likewise, the first experiment in this study has shown the ATP8A2 levels decreased transiently and restored within 10 days after the end of LPS administration (Fig.1). Therefore, the animals were killed after finishing behavioral tasks by over-anesthetized without investigating their PFC ATP8A2 levels or peripheral/cerebral cytokines in adulthood. Understandably, a transient ATP8A2 decrease in PFC might mediate a delayed

517 depressive-like behavior phenotype due to the existing theory of early-life
518 programming (Dinel et al., 2014; Karrow, 2006), saying that the brain is susceptible to
519 external stimuli, such as immune activation, which modulates the course of normal
520 brain development.

521 It has been reported that sex could affect the outcomes in behavior development by
522 itself or combining neonatal immune activation (Cai et al., 2016), which is confirmed
523 by the current study due to the observed between-sexes effects in FST and TST tasks
524 performances (Supplementary Fig.2). However, the PFC ATP8A2 expression and
525 cytokine levels both in blood and in PFC have not been significantly influenced by the
526 sex factor tested at PND11 (Supplementary Fig.1). This may be because the sex factor
527 exerts its effects mainly by gonadal hormones. These endocrine sex differences often
528 come to be obvious from the beginning of puberty and these hormonal disparities
529 contribute to the emerging sex differences in the brain (Cai et al., 2016). Further study
530 is required to address whether the sex factor makes a difference in ATP8A2
531 expression in the brain during puberty as well as adulthood.

532 In sum, our current research demonstrates that neonatal LPS exposure induces
533 ATP8A2 down-regulation in PFC and depressive-like behaviors in mice through
534 increasing the IFN-γ level.

535

536 **Competing interests**

537 The authors declare that there are no conflicts of interest.

Acknowledgments

We thank Mr. Taoqi Tao (ORCID: 0000-0002-2770-9568, from GDPU), Mrs. Yinyin Xie (ORCID: 0000-0002-5858-3873, from GDPU) for their valuable discussions and help with this investigation. The work was supported by the starting fund for high-level talent introduction into Guangdong Pharmaceutical University (No.51355093), the National Natural Science Foundation of China (No.31600836), the Innovation and University Promotion Project of Guangdong Pharmaceutical University Through No. 2017KCXTD020, the National Natural Science Foundation of China (No.81901524), the Natural Science Foundation of Guangdong Province (No.2018A030313579).

References

Aaron, P.A., Jamklang, M., Uhrig, J.P., and Gelli, A. (2018). The blood-brain barrier internalises Cryptococcus neoformans via the EphA2-tyrosine kinase receptor. Cell Microbiol *20*.

Andersen, J.P., Vestergaard, A.L., Mikkelsen, S.A., Mogensen, L.S., Chalat, M., and Molday, R.S. (2016). P4-ATPases as Phospholipid Flippases-Structure, Function, and Enigmas. Front Physiol *7*, 275.

Bilbo, S.D., and Schwarz, J.M. (2012). The immune system and developmental programming of brain and behavior. Front Neuroendocrinol *33*, 267-286.

Brandon, N.J., and Sawa, A. (2011). Linking neurodevelopmental and synaptic theories of mental illness through DISC1. Nat Rev Neurosci *12*, 707-722.

561 Cai, K.C., van Mil, S., Murray, E., Mallet, J.F., Matar, C., and Ismail, N. (2016). Age and sex
562 differences in immune response following LPS treatment in mice. Brain Behav Immun *58*,
563 327-337.

564 Campos, A.C., Vaz, G.N., Saito, V.M., and Teixeira, A.L. (2014). Further evidence for the role
565 of interferon-gamma on anxiety- and depressive-like behaviors: involvement of hippocampal
566 neurogenesis and NGF production. Neurosci Lett *578*, 100-105.

567 Chen, J., Wang, Z., Zhang, S., Ai, Q., Chu, S., and Chen, N.-h. (2017). Possible target-related
568 proteins of stress-resistant rats suggested by label-free proteomic analysis. RSC Advances *7*,
569 40957-40964.

570 Choi, H., Andersen, J.P., and Molday, R.S. (2019). Expression and functional characterization
571 of missense mutations in ATP8A2 linked to severe neurological disorders. Hum Mutat *40*,
572 2353-2364.

573 Coleman, J.A., Kwok, M.C., and Molday, R.S. (2009). Localization, purification, and functional
574 reconstitution of the P4-ATPase Atp8a2, a phosphatidylserine flippase in photoreceptor disc
575 membranes. J Biol Chem *284*, 32670-32679.

576 Coleman, J.A., and Molday, R.S. (2011). Critical role of the beta-subunit CDC50A in the stable
577 expression, assembly, subcellular localization, and lipid transport activity of the P4-ATPase
578 ATP8A2. J Biol Chem *286*, 17205-17216.

579 Depino, A.M. (2015). Early prenatal exposure to LPS results in anxiety- and
580 depression-related behaviors in adulthood. Neuroscience *299*, 56-65.

581 Dinel, A.L., Joffre, C., Trifilieff, P., Aubert, A., Foury, A., Le Ruyet, P., and Laye, S. (2014).
582 Inflammation early in life is a vulnerability factor for emotional behavior at adolescence and for

583 lipopolysaccharide-induced spatial memory and neurogenesis alteration at adulthood. J
584 Neuroinflammation *11*, 155.

585 Doosti, M.H., Bakhtiari, A., Zare, P., Amani, M., Majidi-Zolbanin, N., Babri, S., and Salari, A.A.
586 (2013). Impacts of early intervention with fluoxetine following early neonatal immune activation
587 on depression-like behaviors and body weight in mice. Prog Neuropsychopharmacol Biol
588 Psychiatry *43*, 55-65.

589 Gupta, R., Gupta, K., Tripathi, A.K., Bhatia, M.S., and Gupta, L.K. (2016). Effect of Mirtazapine
590 Treatment on Serum Levels of Brain-Derived Neurotrophic Factor and Tumor Necrosis
591 Factor-alpha in Patients of Major Depressive Disorder with Severe Depression. Pharmacology
592 *97*, 184-188.

593 Haba, R., Shintani, N., Onaka, Y., Wang, H., Takenaga, R., Hayata, A., Baba, A., and
594 Hashimoto, H. (2012). Lipopolysaccharide affects exploratory behaviors toward novel objects
595 by impairing cognition and/or motivation in mice: Possible role of activation of the central
596 amygdala. Behav Brain Res *228*, 423-431.

597 Hansen-Pupp, I., Harling, S., Berg, A.C., Cilio, C., Hellstrom-Westas, L., and Ley, D. (2005).
598 Circulating interferon-gamma and white matter brain damage in preterm infants. Pediatr Res
599 *58*, 946-952.

600 Hashimoto, K. (2015). Inflammatory biomarkers as differential predictors of antidepressant
601 response. Int J Mol Sci *16*, 7796-7801.

602 Karrow, N.A. (2006). Activation of the hypothalamic-pituitary-adrenal axis and autonomic
603 nervous system during inflammation and altered programming of the neuroendocrine-immune
604 axis during fetal and neonatal development: lessons learned from the model inflammagen,

lipopolysaccharide. Brain Behav Immun *20*, 144-158.

Klimstra, W.B., Ryman, K.D., Bernard, K.A., Nguyen, K.B., Biron, C.A., and Johnston, R.E. (1999). Infection of neonatal mice with sindbis virus results in a systemic inflammatory response syndrome. J Virol *73*, 10387-10398.

Kohler, O., Benros, M.E., Nordentoft, M., Farkouh, M.E., Iyengar, R.L., Mors, O., and Krogh, J. (2014). Effect of anti-inflammatory treatment on depression, depressive symptoms, and adverse effects: a systematic review and meta-analysis of randomized clinical trials. JAMA Psychiatry *71*, 1381-1391.

Laumet, G., Edralin, J.D., Chiang, A.C., Dantzer, R., Heijnen, C.J., and Kavelaars, A. (2018). Resolution of inflammation-induced depression requires T lymphocytes and endogenous brain interleukin-10 signaling. Neuropsychopharmacology *43*, 2597-2605.

Lee, J.W., Lee, Y.K., Yuk, D.Y., Choi, D.Y., Ban, S.B., Oh, K.W., and Hong, J.T. (2008). Neuro-inflammation induced by lipopolysaccharide causes cognitive impairment through enhancement of beta-amyloid generation. J Neuroinflammation *5*, 37.

Liang, M., Zhong, H., Rong, J., Li, Y., Zhu, C., Zhou, L., and Zhou, R. (2019). Postnatal Lipopolysaccharide Exposure Impairs Adult Neurogenesis and Causes Depression-like Behaviors Through Astrocytes Activation Triggering GABAA Receptor Downregulation. Neuroscience *422*, 21-31.

Miller, A.J., Roman, B., and Norstrom, E. (2016). A method for easily customizable gradient gel electrophoresis. Anal Biochem *509*, 12-14.

Myers-Schulz, B., and Koenigs, M. (2012). Functional anatomy of ventromedial prefrontal cortex: implications for mood and anxiety disorders. Mol Psychiatry *17*, 132-141.

627 O'Reilly, B., Vander, A.J., and Kluger, M.J. (1988). Effects of chronic infusion of
628 lipopolysaccharide on food intake and body temperature of the rat. Physiol Behav *42*, 287-291.
629 Pokryszko-Dragan, A., Frydecka, I., Kosmaczewska, A., Ciszak, L., Bilinska, M., Gruszka, E.,
630 Podemski, R., and Frydecka, D. (2012). Stimulated peripheral production of interferon-gamma
631 is related to fatigue and depression in multiple sclerosis. Clin Neurol Neurosurg *114*,
632 1153-1158.
633 Ross, A.E., Marchionni, L., Vuica-Ross, M., Cheadle, C., Fan, J., Berman, D.M., and Schaeffer,
634 E.M. (2011). Gene expression pathways of high grade localized prostate cancer. Prostate *71*,
635 1568-1577.
636 Shaw, K.N., Commins, S., and O'Mara, S.M. (2001). Lipopolysaccharide causes deficits in
637 spatial learning in the watermaze but not in BDNF expression in the rat dentate gyrus. Behav
638 Brain Res *124*, 47-54.
639 Shulzhenko, N., Dong, X., Vyshenska, D., Greer, R.L., Gurung, M., Vasquez-Perez, S.,
640 Peremyslova, E., Sosnovtsev, S., Quezado, M., Yao, M.*, et al.* (2018). CVID enteropathy is
641 characterized by exceeding low mucosal IgA levels and interferon-driven inflammation
642 possibly related to the presence of a pathobiont. Clin Immunol *197*, 139-153.
643 Walker, A.K., Budac, D.P., Bisulco, S., Lee, A.W., Smith, R.A., Beenders, B., Kelley, K.W., and
644 Dantzer, R. (2013). NMDA receptor blockade by ketamine abrogates
645 lipopolysaccharide-induced depressive-like behavior in C57BL/6J mice.
646 Neuropsychopharmacology *38*, 1609-1616.
647 Wang, Z., Li, W., Chen, J., Shi, H., Zhao, M., You, H., Rao, C., Zhan, Y., Yang, Y., and Xie, P.
648 (2016). Proteomic analysis reveals energy metabolic dysfunction and neurogenesis in the

649 prefrontal cortex of a lipopolysaccharide-induced mouse model of depression. Mol Med Rep
650 *13*, 1813-1820.
651 Wong, D., Dorovini-Zis, K., and Vincent, S.R. (2004). Cytokines, nitric oxide, and cGMP
652 modulate the permeability of an in vitro model of the human blood-brain barrier. Exp Neurol
653 *190*, 446-455.
654 Xiong, B., Li, A., Lou, Y., Chen, S., Long, B., Peng, J., Yang, Z., Xu, T., Yang, X., Li, X.*, et al.*
655 (2017). Precise Cerebral Vascular Atlas in Stereotaxic Coordinates of Whole Mouse Brain.
656 Front Neuroanat *11*, 128.
657 Xu, Q., Yang, G.Y., Liu, N., Xu, P., Chen, Y.L., Zhou, Z., Luo, Z.G., and Ding, X. (2012).
658 P4-ATPase ATP8A2 acts in synergy with CDC50A to enhance neurite outgrowth. FEBS Lett
659 *586*, 1803-1812.
660 Yang, J., Qi, F., Gu, H., Zou, J., Yang, Y., Yuan, Q., and Yao, Z. (2016). Neonatal BCG
661 vaccination of mice improves neurogenesis and behavior in early life. Brain Res Bull *120*,
662 25-33.
663 Zhu, X., Libby, R.T., de Vries, W.N., Smith, R.S., Wright, D.L., Bronson, R.T., Seburn, K.L.,
664 and John, S.W. (2012). Mutations in a P-type ATPase gene cause axonal degeneration. PLoS
665 Genet *8*, e1002853.
666
667
668
669
670

Legends

Fig.1. Neonatal LPS exposure induced a transiently down-regulated expression of ATP8A2 in the PFC in mice. (A) Representative results for the Western blot analysis of ATP8A2. **(B)** The relative quantification of ATP8A2 in each group of mice was normalized using the level of β-actin. Data are expressed as means ± SEM. Randomly block design ANOVA; n = 6/group; * $p < 0.05$; *** $p < 0.001$.

Fig.2. Neonatal LPS exposure induced a down-regulated expression of ATP8A2 accompanied by inflammation both in periphery and in PFC in mice.

(A) Representative results for the Western blot analysis of ATP8A2. **(B)** The relative quantification of ATP8A2 in each group of mice was normalized using the level of β-actin. **(C-J)** The bars represent the average levels of IFN-γ, IL-1β, IL-6, TNF-α in the serum and IFN-γ ，IL-1β, IL-6, TNF-α in the PFC. Data are expressed as means ± SEM. Randomly block design ANOVA; n = 9/group; * $p < 0.05$; **$p < 0.01$; *** $p < 0.001$.

Fig.3. The correlation of PFC ATP8A2 level with the serum and PFC levels of pro-inflammatory cytokines in mice. (A) The positive negative correlation of the PFC IFN-γ level with the ATP8A2 expression level in LPS-treated mice. **(B-D)** Correlation analyses between the PFC IL-1β, IL-6 and TNF-α levels and the level of ATP8A2 LPS-treated mice**. (E)** The positive negative correlation of the serum IFN-γ level with the ATP8A2 expression level in LPS-treated mice. **(F-H)** Correlation analyses between the serum IL-1β, IL-6 and TNF-α levels and the level of ATP8A2

692 LPS-treated mice**.** *n* = 15 per analysis ; *Pearson*'s correlation analysis.

693 **Fig.4. Western blot analyses showed that IFN-γ mediated the PFC ATP8A2**
694 **down-regulation caused by neonatal LPS exposure.**

695 **(A-B)** The mean levels of IFN-γ in the serum and PFC were shown from the
696 experiment carried out to determine the optimal dosage of anti-IFN-γ neutralizing
697 mAb. **(C-D)** The mean levels of IFN-γ in the serum and PFC were shown from the
698 IFN-γ-blocking experiment. **(E)** The relative quantification of ATP8A2 in each group
699 of mice was normalized using the level of β-actin. **(F)** Representative results for the
700 Western blot analysis of ATP8A2. Data are expressed as means ± SEM. Randomly
701 block design ANOVA followed by Tukey's *post hoc* test; n = 8/group; $^{**}p < 0.01$;
702 *** $p < 0.001$; n.s., no significant. anti-IFN-γ(0.6), the anti-IFN-γ dosage of 0.6
703 mg/kg body weight.

704 **Fig.5. Immunofluorescence analyses showed that IFN-γ mediated the PFC**
705 **ATP8A2 down-regulation caused by neonatal LPS exposure. (A-C)** Representative
706 immunofluorescence staining results in the PFC for ATP8A2(red)/NeuN(green)
707 co-labeling in CON group (A), LPS group (B) and LPS+anti-IFN-γ(0.6) group (C).
708 **(E-F)** Exhibition of the single red channel that shows ATP8A2 signal of the same
709 micrographs shown in (A), (B), (C), respectively. **(G-I)** Representative high
710 magnificent photos show the immunofluorescence staining results in the PFC for
711 ATP8A2/NeuN co-labeling. Thick arrows indicate ATP8A2/NeuN co-labeling cells.
712 Thin arrows indicate NeuN single labeling cells. **(J)** The larger scope shows the

location in PFC where the photos shown in (G-I) come from. **(K)** Bars represent mean fluorescence intensity of the signal of immunofluorescence staining for ATP8A2 in each group. **(I)** Bars represent mean numbers of ATP8A2/NeuN co-labeling cells in unilateral PFC in each group. Data are expressed as means ± SEM. Randomly block design ANOVA followed by Tukey's *post hoc* test; n = 6/group; *** $p < 0.001$; anti-IFN-γ(0.6), the anti-IFN-γ dosage of 0.6 mg/kg body weight. Scale bar in (A-F), 300 μm; in (G-I), 10 μm; in (J), 200 μm.

Fig.6. IFN-γ plays an important role in depressive-like behaviors in adulthood induced by neonatal LPS exposure. (A) Bars represent the mean immobility time of mice in FST of each group. **(I)** Bars represent the mean immobility time of TST in each group. The data represent the mean ± SEM; randomly block design ANOVA followed by Tukey's *post hoc* test; n = 12/group; *$p < 0.05$, **$p < 0.01$, ***$p < 0.001$; anti-IFN-γ(0.6), the anti-IFN-γ dosage of 0.6 mg/kg body weight.

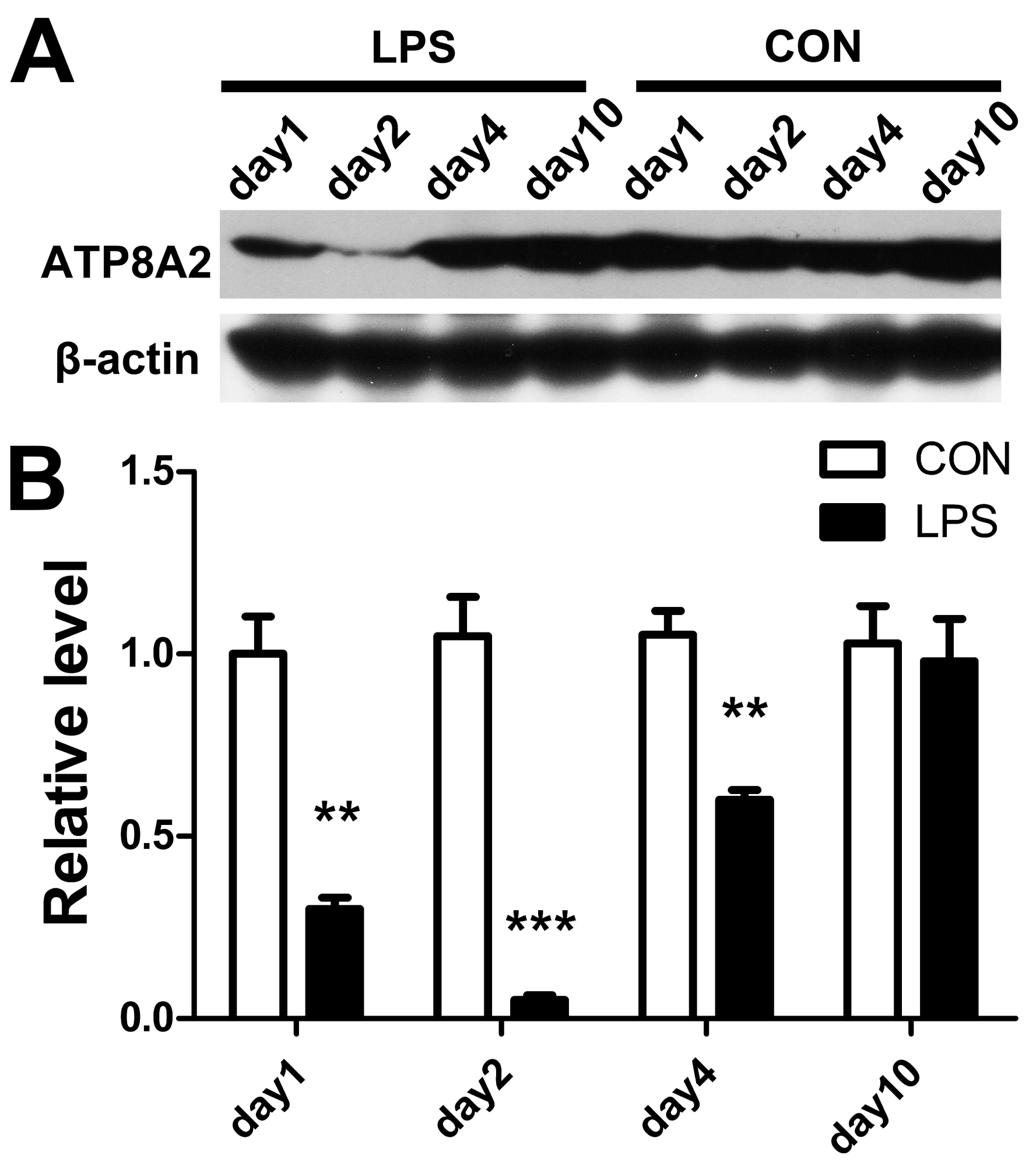
A
LPS
CON
day1
day2
day4
day10
day1
day2
day4
day10
ATP8A2
β-actin
B
CON
LPS
Relative level
1.5
1.0
0.5
0.0
**
***
**
day1
day2
day4
day10

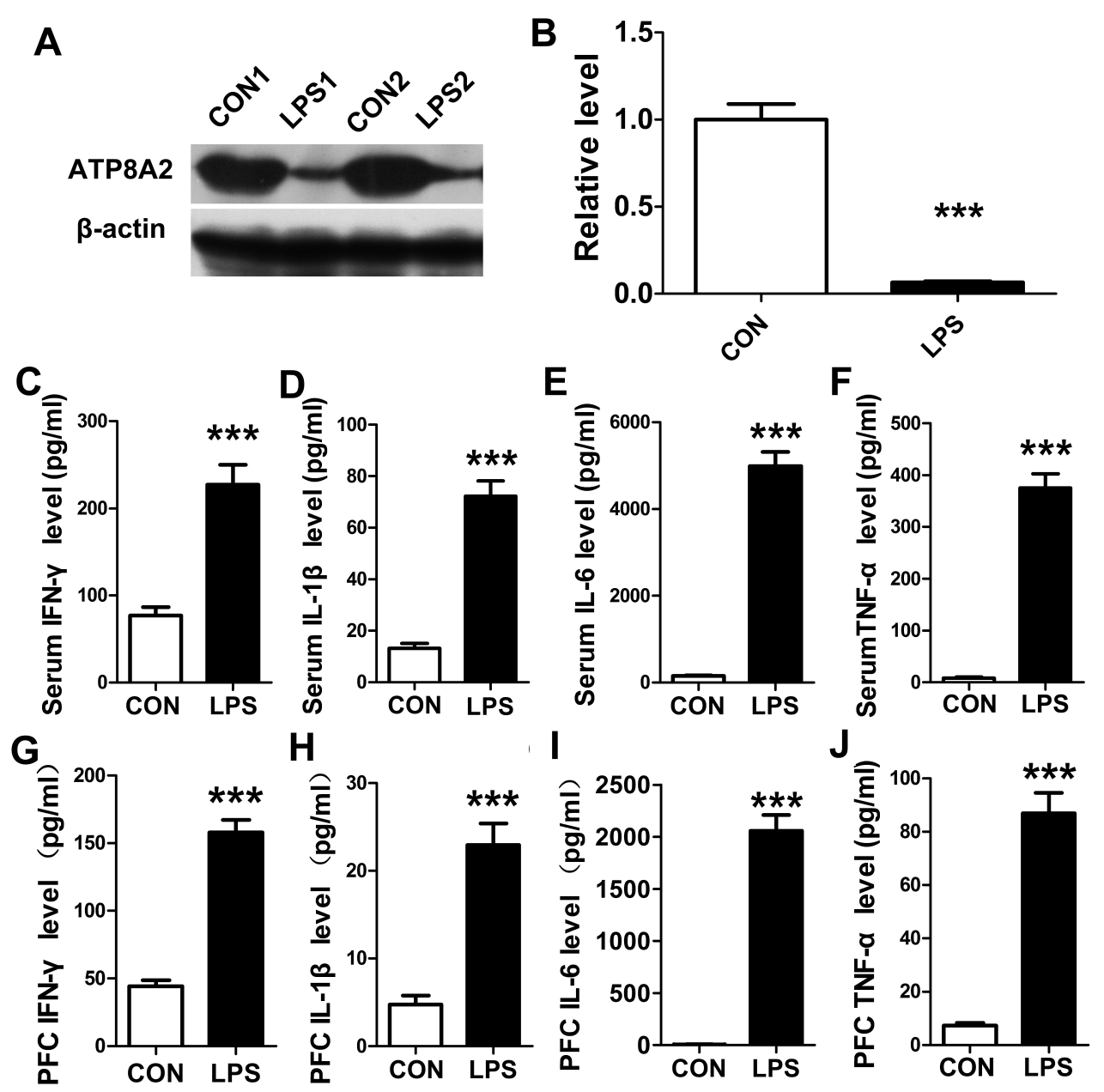
A
CON1
LPS1
CON2
LPS2
ATP8A2
β-actin
B
Relative level
1.5
1.0
0.5
0.0
***
CON
LPS
C
Serum IFN-γ level (pg/ml)
300
200
100
0
***
CON
LPS
D
Serum IL-1β level (pg/ml)
100
80
60
40
20
0
***
CON
LPS
E
Serum IL-6 level (pg/ml)
6000
4000
2000
0
***
CON
LPS
F
SerumTNF-α level (pg/ml)
500
400
300
200
100
0
***
CON
LPS
G
PFC IFN-γ level (pg/ml)
200
150
100
50
0
***
CON
LPS
H
PFC IL-1β level (pg/ml)
30
20
10
0
***
CON
LPS
I
PFC IL-6 level (pg/ml)
2500
2000
1500
1000
500
0
***
CON
LPS
J
PFC TNF-α level (pg/ml)
100
80
60
40
20
0
***
CON
LPS

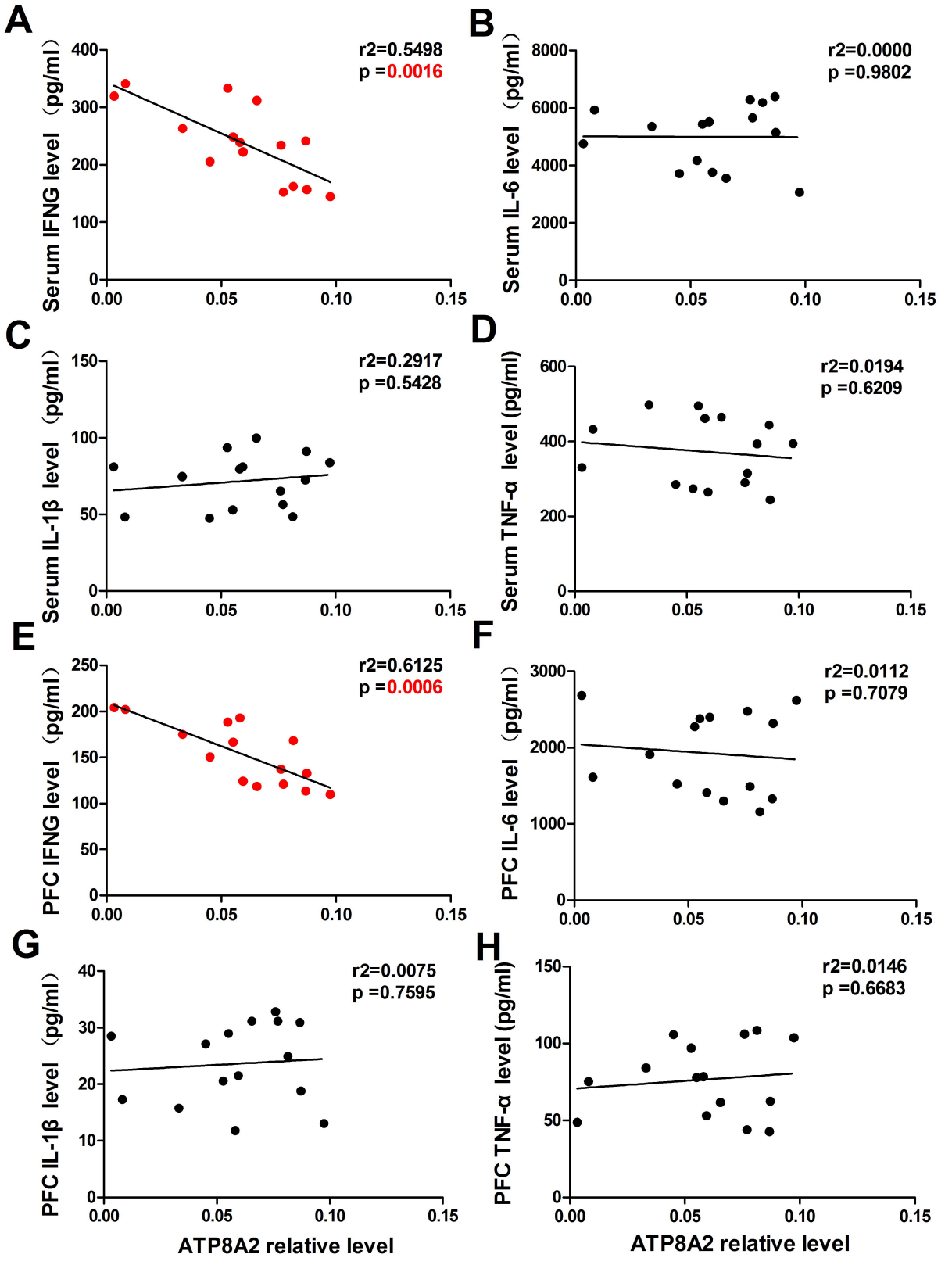
A
r2=0.5498
p =0.0016
Serum IFNG level （pg/ml）
B
r2=0.0000
p =0.9802
Serum IL-6 level （pg/ml）
C
r2=0.2917
p =0.5428
Serum IL-1β level （pg/ml）
D
r2=0.0194
p =0.6209
Serum TNF-α level (pg/ml)
E
r2=0.6125
p =0.0006
PFC IFNG level （pg/ml）
F
r2=0.0112
p =0.7079
PFC IL-6 level （pg/ml）
G
r2=0.0075
p =0.7595
PFC IL-1β level （pg/ml）
H
r2=0.0146
p =0.6683
PFC TNF-α level (pg/ml)
ATP8A2 relative level
ATP8A2 relative level

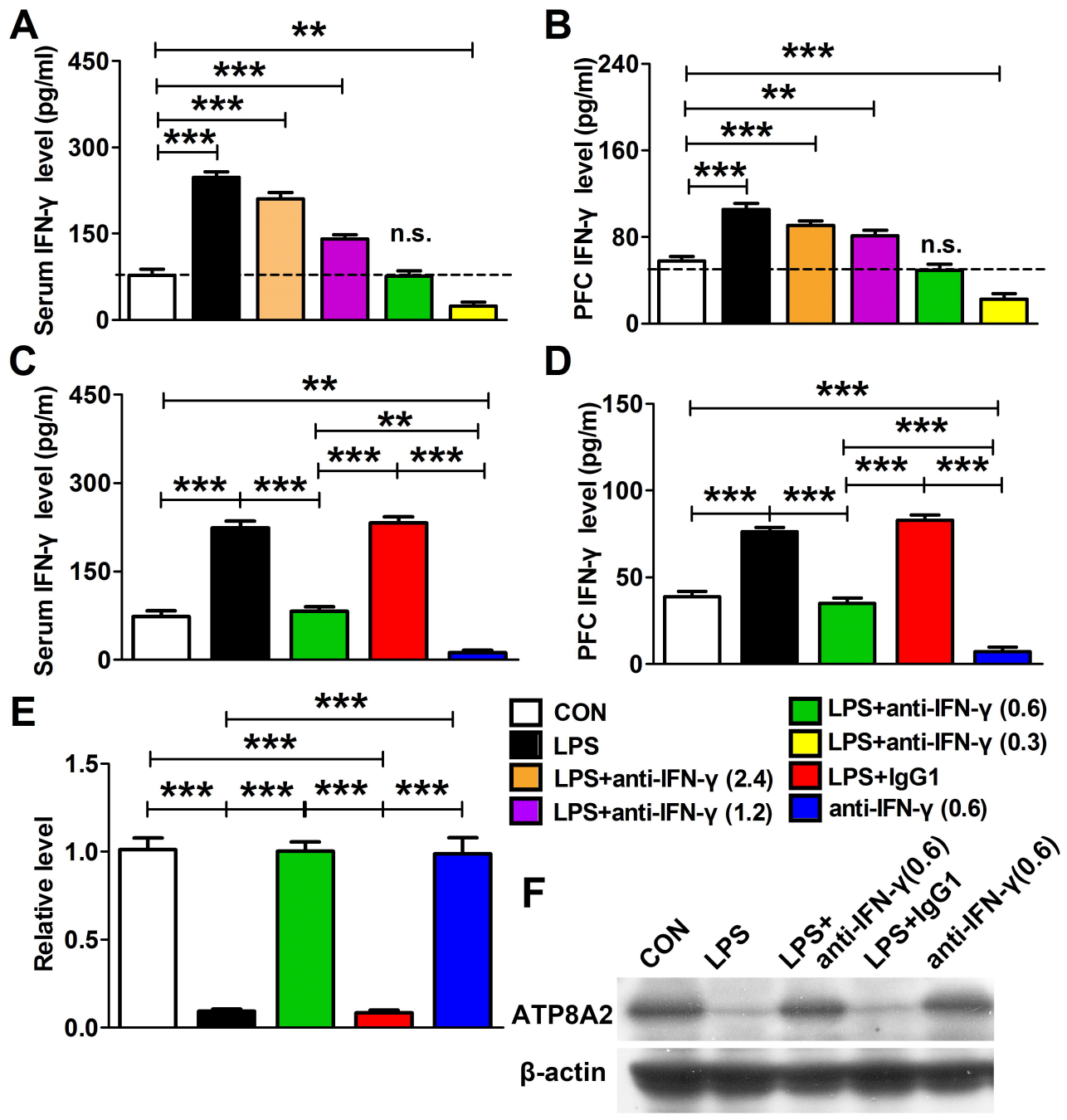
A
Serum IFN-γ level (pg/ml)
450
300
150
0
**
***
***
***
n.s.
B
PFC IFN-γ level (pg/ml)
240
160
80
0
***
**
***
***
n.s.
C
Serum IFN-γ level (pg/m)
450
300
150
0
**
**
***
***
***
***
D
PFC IFN-γ level (pg/m)
150
100
50
0
***
***
***
***
***
E
Relative level
1.5
1.0
0.5
0.0
***
***
***
***
***
***
CON
LPS
LPS+anti-IFN-γ (2.4)
LPS+anti-IFN-γ (1.2)
LPS+anti-IFN-γ (0.6)
LPS+anti-IFN-γ (0.3)
LPS+IgG1
anti-IFN-γ (0.6)
F
CON
LPS
LPS+ anti-IFN-γ(0.6)
LPS+IgG1
anti-IFN-γ(0.6)
ATP8A2
β-actin

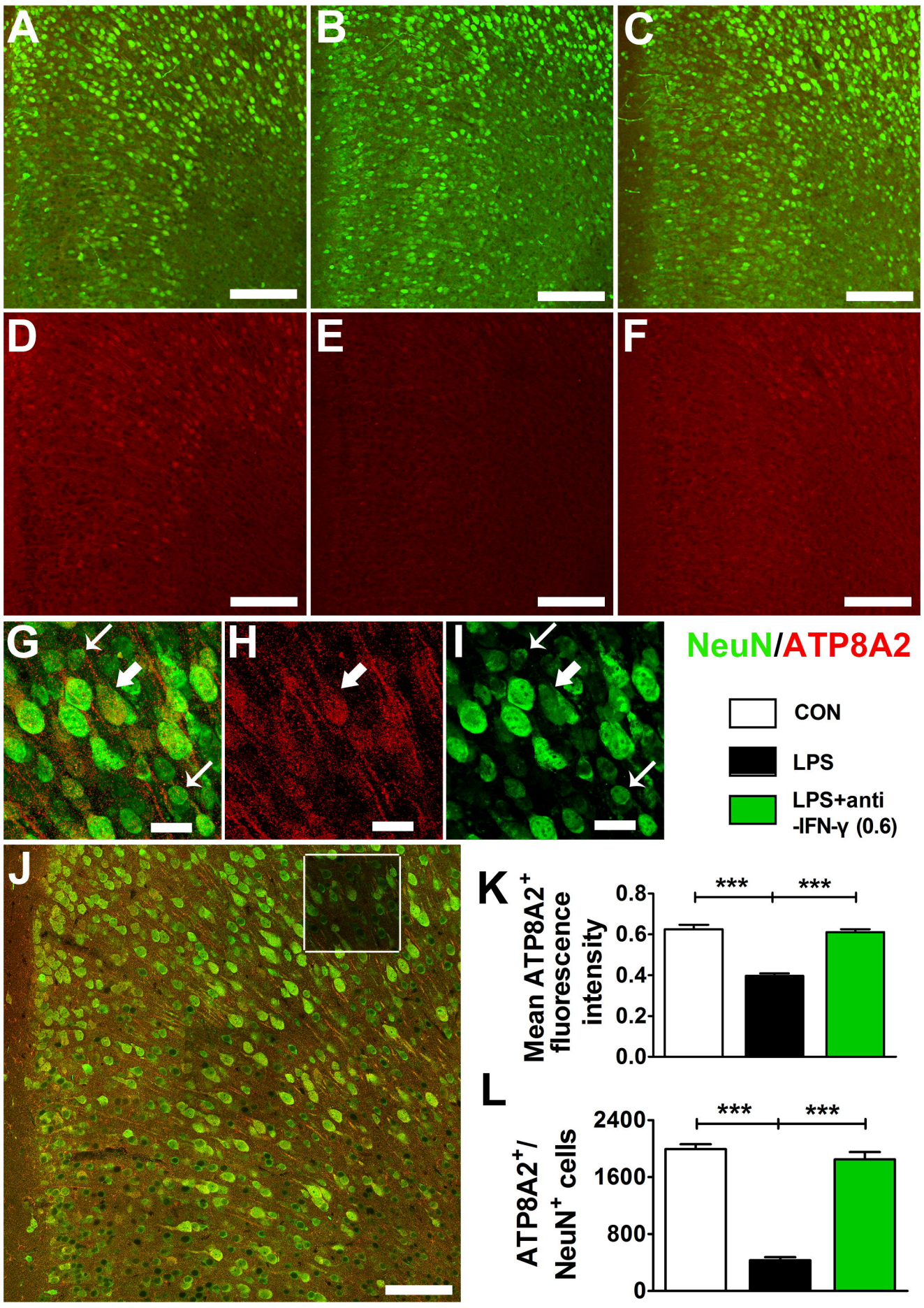
A
B
C
D
E
F
G
H
I
NeuN/ATP8A2
CON
LPS
LPS+anti
-IFN-γ (0.6)
J
K
Mean ATP8A2+
fluorescence
intensity
0.8
0.6
0.4
0.2
0.0
***
***
L
ATP8A2+/
NeuN+ cells
2400
1600
800
0
***
***

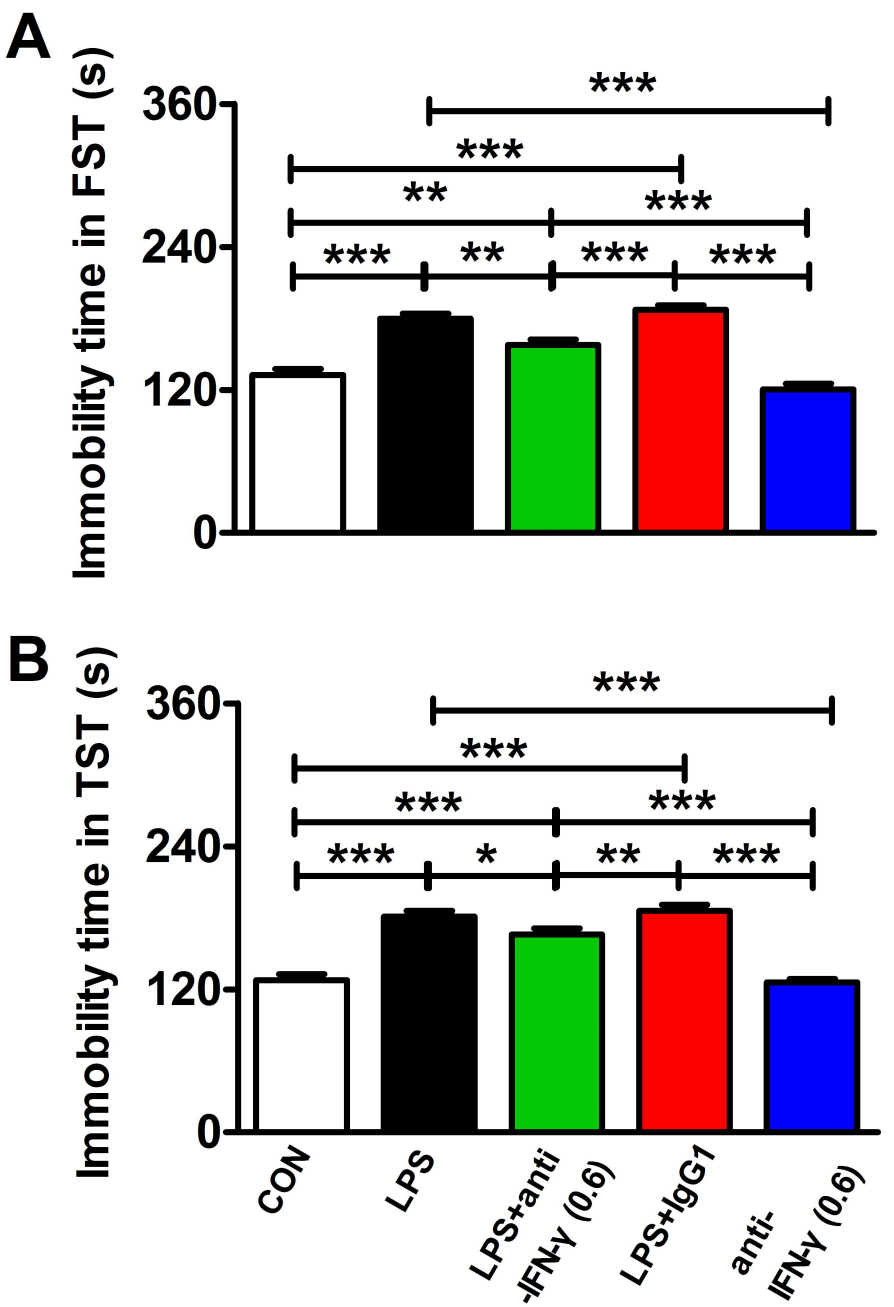
A
Immobility time in FST (s)
360
240
120
0
***
***
**
***
***
**
***
***
B
Immobility time in TST (s)
360
240
120
0
***
***
***
***
***
*
**
***
CON
LPS
LPS+anti -IFN-γ (0.6)
LPS+IgG1
anti- IFN-γ (0.6)